

## Ultraviolet photoelectron spectra of $Ce_2@C_{80}$ and $La_2@C_{80}$



Takafumi Miyazaki<sup>a,\*</sup>, Sosuke Okita<sup>a</sup>, Tomona Ohta<sup>a</sup>, Hajime Yagi<sup>a</sup>, Ryohei Sumii<sup>b,c</sup>, Haruya Okimoto<sup>d</sup>, Yasuhiro Ito<sup>d</sup>, Hisanori Shinohara<sup>d</sup>, Shojun Hino<sup>a</sup>

<sup>a</sup> Graduate School of Science and Engineering, Ehime University, Matsuyama 790-8577, Japan

<sup>b</sup> Institutes for Molecular Science, Okazaki 444-858, Japan

<sup>c</sup> Research Center for Materials Science, Nagoya University, Chikusa-ku, Nagoya 464-8602, Japan

<sup>d</sup> Graduate School of Science, Nagoya University, Chikusa-ku, Nagoya 464-8602, Japan

### ARTICLE INFO

#### Article history:

Received 27 August 2014

In final form 3 December 2014

Available online 11 December 2014

#### Keywords:

Endohedral fullerenes

La and Ce atoms encapsulated  $C_{80}$  cage

Electronic structure

Ultraviolet photoelectron spectroscopy

X-ray photoelectron spectroscopy

### ABSTRACT

Ultraviolet photoelectron spectra (UPS) of  $C_{80}$ - $I_h$  cage endohedral fullerenes,  $La_2@C_{80}$  and  $Ce_2@C_{80}$  were measured using a synchrotron radiation light source. The spectral onset energy of  $La_2@C_{80}$  and  $Ce_2@C_{80}$  is around 0.8–0.9 eV, which is smaller than that of empty  $C_{80}$ - $I_h$ . The UPS of these endohedral fullerenes are almost identical and are discussed with an aid of density functional theory (DFT) calculation. Simulation spectra calculated with using the results of the DFT calculations on an optimized structure starting from  $D_{3d}$  geometry reproduces the UPS of  $La_2@C_{80}$  and  $Ce_2@C_{80}$  very well, which supports the theoretically proposed structure.

© 2014 Elsevier B.V. All rights reserved.

### 1. Introduction

Fullerene cages often encapsulate metal atoms and  $C_{82}$  cage seems to be the most favorable cage in which metal atoms are entrapped [1]. However, other cages also encapsulate metal atoms although their production yield from direct current arc discharge of metal oxide/carbon composite rods is not so high compared with that of  $C_{82}$  endohedral fullerenes. Among other cage endohedral fullerenes,  $C_{80}$  endohedral fullerenes attract attention because of the reasons such as (a) empty  $I_h$ - $C_{80}$  is not stable and cannot be isolated [2] but it becomes stable upon encapsulation of metal atoms [3], (b)  $I_h$ - $C_{80}$  has the same symmetry as  $C_{60}$  [4] which exhibits many interesting solid state properties like superconductivity [5] and ferromagnetism [6]. Although early stage X-ray diffraction analysis combined with maximum entropy method (MEM) [7] suggested  $I_h$ - $La_2@C_{80}$  cage, theoretical calculations [4,8–12] revealed that metal atoms entrapped  $I_h$ - $C_{80}$  did not retain the original symmetry and encapsulation of metal atoms induced the degradation of symmetry. Crystallographic structure of a  $La_2@C_{80}$  adduct also supported this conclusion that the encapsulation of metal atoms is favorable for the stability of the fullerene cage [13].

Early theoretical calculation on  $La_2@C_{80}$  suggested that entrapped two La atoms rotated in the  $D_{2h}$ - $C_{80}$  cage [8]. X-ray crystallographic analysis of its adduct,  $La_2@C_{80}(CH_2)(C_6H_5)_3N$ , revealed

that the rotation was frozen [4]. {The oxidation state of entrapped La in both  $La_2@C_{80}$  [8] and the adduct [13] was calculated by DFT calculation to be +3.} On the other hand, vibrational mode analysis using DFT calculation of  $La_2@C_{80}$  suggested  $D_{3d}$  symmetry that is the global minimum in total energy [10]. This proposal was questioned by recent DFT calculations [11,12] that supported  $D_{2h}$  geometry; using relativistic basis sets could be a crucial factor to a favor of  $D_{2h}$ .

The argument on the geometry of  $I_h$ - $C_{80}$  endohedral fullerenes did not stop at this point. Another  $I_h$ -cage endohedral fullerene,  $Ce_2@C_{80}$ , was isolated [14] and its predicted geometry was not  $D_{2h}$  but  $D_{3d}$  [12]. The reason of  $Ce_2@C_{80}$  having  $D_{3d}$  geometry was attributed to specific bonding condition of Ce atoms to the cage: they bonded to C atoms on the opposite side of  $C_6$  axis of  $C_{80}$ .

We have been measuring ultraviolet photoelectron spectra (UPS) of endohedral fullerenes and reported the most plausible cage geometry by a comparison of the UPS [15–17]. There is an empirical rule for endohedral  $C_{82}$  fullerenes that their electronic structure is essentially governed by the cage structure (symmetry) and the amounts of electrons transferred from the entrapped species. Thus, if one obtains analogous UPS from different endohedral fullerenes, both their cage structure (symmetry) and the amounts of transferred electrons should be almost identical. Furthermore, we have compared the UPS of endohedral fullerenes with theoretically obtained simulated spectra [18–22]. There is no theoretical reasoning that Kohn–Sham orbital energies obtained from DFT calculation is compatible with Koopmans' theorem, but Janak's theorem is analog to Koopmans' theorem in DFT calculation; that

\* Corresponding author. Fax: +81 89 927 9942.

E-mail address: [miyazaki@eng.ehime-u.ac.jp](mailto:miyazaki@eng.ehime-u.ac.jp) (T. Miyazaki).

Kohn–Sham orbital energies correspond the highest occupied and the lowest unoccupied molecular orbitals energy levels. Further, it has been found that simulated spectra generated from Kohn–Sham orbital energies reproduce the UPS very well and the comparison was helpful to estimate the cage geometry. The UPS of  $\text{La}_2@C_{80}$  was tried to measure but any specific structure which was considered to be characteristic to the UPS of fullerenes was not observed [23]. Therefore, the comparison between the UPS of  $\text{La}_2@C_{80}$  and the simulated spectra was impossible.

We succeeded to measure the UPS of  $\text{La}_2@C_{80}$  and  $\text{Ce}_2@C_{80}$ . In this article their UPS will be presented and they are compared with simulated spectra obtained from DFT calculation. Their possible geometry will be provided to settle the  $D_{2h}$  or  $D_{3d}$  argument on the  $I_h$  cage endohedral fullerenes.

## 2. Experimental and calculation methods

The synthesis and isolation of  $\text{La}_2@C_{80}$  is reported in Ref. [7].  $\text{Ce}_2@C_{80}$  was also obtained with the same method. Soot containing  $\text{M}_2@C_{80}$  ( $M = \text{La}$  or  $\text{Ce}$ ) was produced by direct-current arc heating of a  $\text{M}_2\text{O}_3/\text{graphite}$  composite rod in a He atmosphere. The detail of preparation was described in Ref. [24]. Samples for the photoelectron measurements were prepared by vacuum sublimation of the endohedral fullerenes onto a gold-deposited molybdenum disk. Sublimation was conducted using a resistive heating quartz crucible in a preparation vacuum chamber directly attached to a photoelectron measurement chamber. The temperature of the crucible during  $\text{La}_2@C_{80}$  and  $\text{Ce}_2@C_{80}$  sublimation was about 850–870 K. The pressure of the chamber during the deposition increased to  $2 \times 10^{-6}$  Pa (base pressure before the deposition was less than  $4.0 \times 10^{-7}$  Pa). The thickness of deposited endohedral fullerenes was tried to monitor by a quartz thickness monitor located beside the disk, but because of the collimation of the crucible the reading of the monitor indicated several nm thickness. However, the actual thickness of the film might be several tens of nm, since the gold Fermi edge was not observed after repeated sample deposition.

The UPS were measured using a photoelectron spectrometer at BL8B2 of UVSOR (Ultraviolet Synchrotron Orbital Radiation Facility) at the Institute for Molecular Science. The resolution of the spectrometer was 110 meV. Energy calibration of the spectra was carried out using the Fermi edge of a gold-deposited sample disk before the UPS measurements of  $\text{La}_2@C_{80}$  and  $\text{Ce}_2@C_{80}$ . The spectra were referenced against the Fermi level. The base pressure of the measurement chamber was  $\leq 9.0 \times 10^{-8}$  Pa, and the pressure during the measurement was about  $6.0 \times 10^{-8}$  Pa.

Molecular orbitals of  $\text{La}_2@C_{80}$  and  $\text{Ce}_2@C_{80}$  were calculated with a Gaussian 03 program module. Their geometry was optimized at the Hartree–Fock level using the CEP-31G basis set. Poor correspondence was observed between the UPS and simulated spectra generated by broadening the calculated Eigen values at the Hartree–Fock level with Gaussian functions of 0.2 eV full width at half maximum. The DFT calculation was performed on the optimized structures of  $\text{La}_2@C_{80}$  and  $\text{Ce}_2@C_{80}$  using the B3LYP hybrid functional to obtain the Kohn–Sham orbital energies with basis sets Sapporo-DZP for C atoms and TK/NOSec-V-TZP function for La and Ce atoms [25,26]. Simulated spectra obtained by the same procedure describe above using Kohn–Sham orbital energies reproduced the UPS far better than those obtained from the Hartree–Fock calculation. The simulated spectra in the following text are the result of the DFT calculation.

## 3. Results and discussion

Figs. 1 and 2 show the UPS of  $\text{La}_2@C_{80}$  and  $\text{Ce}_2@C_{80}$  obtained with the incident photon energy indicated beside each spectrum.

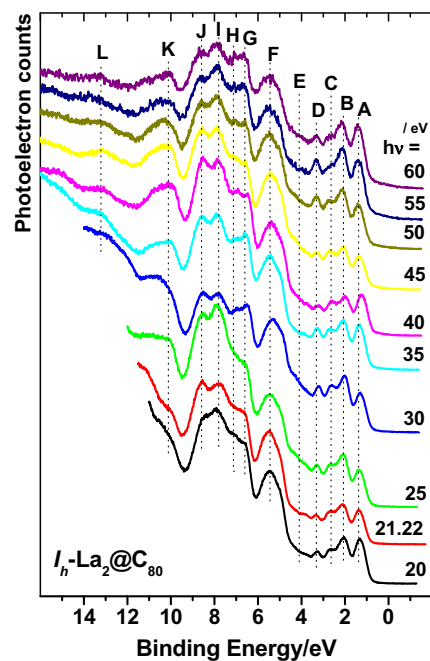


Fig. 1. Incident photon energy dependent ultraviolet photoelectron spectra of  $\text{La}_2@C_{80}$ . Numeric beside each spectrum indicates the energy of the incident photon. Approximate peak positions are indicated with dotted lines.

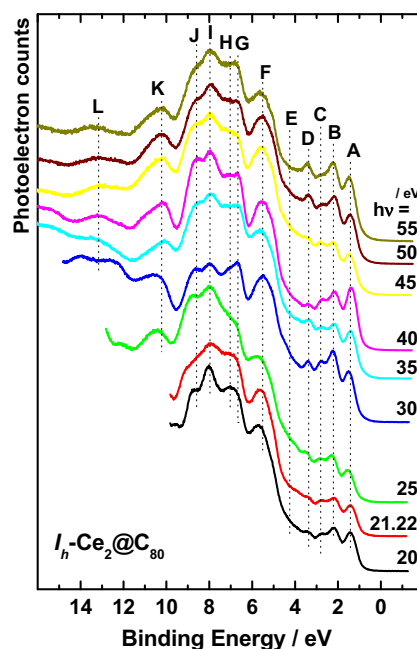


Fig. 2. Incident photon energy dependent ultraviolet photoelectron spectra of  $\text{Ce}_2@C_{80}$ . Numeric beside each spectrum indicates the energy of the incident photon. Approximate peak positions are indicated with dotted lines.

The spectral onset of  $\text{La}_2@C_{80}$  and  $\text{Ce}_2@C_{80}$  was 0.77 and 0.89 eV below the Fermi level, respectively. Except for the onset energy, their UPS are almost identical. There are 12 structures labeled A to L in their UPS. Among them, structure E appears as a shoulder not explicit and structure H appears as a distinct peak in the spectra obtained with the incident photon energy larger than 30 eV. Approximate peak positions of their structures are indicated with dotted lines. As were observed in the UPS of other fullerenes [18–23,27], the relative intensity of these structures oscillates

when the energy of the incident photon is tuned. Because of this intensity oscillation, peak positions deviate slightly in accordance with the incident photon energy change.

Fig. 3 shows the photoelectron spectra of  $\text{La}_2@C_{80}$  and  $\text{Ce}_2@C_{80}$  obtained by 40 eV incident photon energy together with the UPS of empty  $C_{80}$  obtained by 60 eV energy [28]. There is a very poor correspondence between the UPS of  $\text{La}_2@C_{80}$  and  $\text{Ce}_2@C_{80}$ , and the UPS of  $C_{80}$ . Only distinct resemblance among these spectra might be a structure appeared at about 5.5 eV which is a typical structure in the UPS of fullerenes [15–17,19–23] and a broad band between 6.0 and 9.5 eV which is due to  $\sigma$ -electrons constituting fullerene backbone. The UPS of  $\text{La}_2@C_{80}$  and  $\text{Ce}_2@C_{80}$  are almost identical and hard to distinguish them. Structures labeled A–H of  $\text{Ce}_2@C_{80}$  appear at deeper binding energy side by about 0.2 eV than corresponding ones of  $\text{La}_2@C_{80}$ . Their relative intensity is almost the same. On the other hand, structures labeled I–L appear at the same binding energy and there is a slight change in the relative intensity of structures I and J. Resemblance of the UPS means that these two endohedral fullerenes have analogous electronic structure. Since the electronic structure of endohedral fullerenes strongly depends on the geometry of fullerenes, both cage and entrapped atoms, it is highly plausible that they have the same cage structure. In order to examine the validity of this deduction, their electronic structure was calculated by the DFT method and Gaussian functions.

Two possible geometries of  $M_2@C_{80}$  ( $M = \text{La}, \text{Ce}$ ),  $D_{2h}$  and  $D_{3d}$  have been proposed [4,8–14]. Three initial conformations of metal atoms in  $I_h-C_{80}$  were adapted; (a)  $D_{5d}$  symmetry, two metal atoms were in the  $C_5$  axis of  $I_h-C_{80}$ , (b)  $D_{2h}$  symmetry, they were in the  $C_2$  axis penetrating the center of hexagon rings perpendicular to the mirror plane of  $I_h-C_{80}$  and (c)  $D_{3d}$  symmetry, in the  $C_3$  axis penetrating the center of phenylene rings. Optimized structures retained the same symmetry adapted as the initial geometry. Kohn–Sham orbital energies were obtained using the optimized geometry. Kohn–Sham orbital energies and simulated spectra generated by broadening them by Gaussian functions are shown in Fig. 4 ( $\text{La}_2@C_{80}$ ) and Fig. 5 ( $\text{Ce}_2@C_{80}$ ). The UPS of  $\text{La}_2@C_{80}$  and  $\text{Ce}_2@C_{80}$  obtained with 30 eV excitation energy are also shown for comparison. The bars in Figs. 4 and 5 indicate the calculated ionization

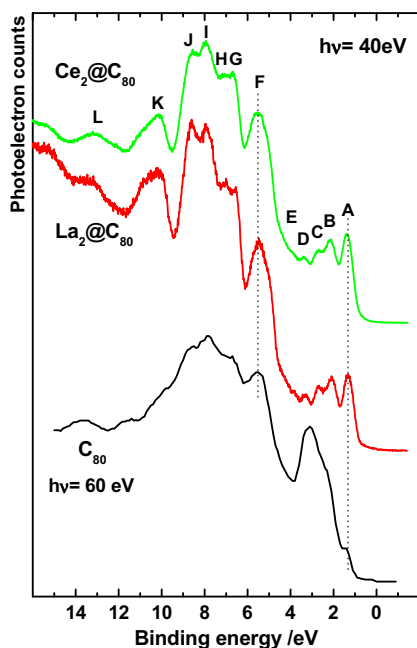


Fig. 3. Ultraviolet photoelectron spectra of  $\text{La}_2@C_{80}$  and  $\text{Ce}_2@C_{80}$  obtained with  $h\nu = 30$  eV photon together with the UPS of empty  $C_{80}$  obtained by 60 eV energy.

energies (Eigenvalues of occupied states). Scale of the simulated spectra and Kohn–Sham orbital energies is shifted by 4.4 eV for an easy comparison. Since the similarity between the UPS and the simulated spectra generated from  $D_{5d}$  geometry of  $M_2@C_{80}$  ( $M = \text{La}$  and  $\text{Ce}$ ) was very poor, the structure of these endohedral fullerenes should not be  $D_{5d}$  geometry. Further, the formation energy of this geometry is much larger than that of the most stable one. Therefore, we do not treat this geometry any further in this text. The simulated spectra generated from  $D_{3d}$  and  $D_{2h}$  geometry seem to reproduce the UPS very well; the first four structures A–D are well reproduced and deeper structures F–J are also reproduced reasonably well. There are slight difference in Kohn–Sham orbital energies (indicated by bars) of  $D_{2h}\text{-La}_2@C_{80}$  and  $D_{2h}\text{-Ce}_2@C_{80}$ , but it is so small that the simulated spectra obtained by their convolution do not show any significant difference. Only attractive difference in the simulated spectra might be associated with the position of the HOMO; the HOMO of  $\text{Ce}_2@C_{80}$  appears at slightly shallower than the HOMO-1 or -2, whereas that of  $\text{La}_2@C_{80}$  locates rather close to the HOMO-1. From these data, present findings suggest that the simulated spectra obtained from  $D_{3d}$  geometry reproduced the UPS of  $\text{Ce}_2@C_{80}$  and  $\text{La}_2@C_{80}$  very well. Hence the actual geometry of  $\text{La}_2@C_{80}$  and  $\text{Ce}_2@C_{80}$  might be  $D_{3d}$ .

Fig. 6 shows calculated energy diagrams of  $\text{Ce}_2@C_{80}$ ,  $C_{80}$  of the same cage symmetry and the entrapped Ce atoms. Fig. 7 shows calculated energy diagrams of  $\text{La}_2@C_{80}$ ,  $C_{80}$  of the same cage symmetry and the entrapped La atoms. Wave functions of some frontier orbitals of  $\text{Ce}_2@C_{80}$ ,  $\text{La}_2@C_{80}$  and  $C_{80}$  are also depicted in the figures. The HOMO-3 and HOMO-2 wave functions of  $\text{Ce}_2@C_{80}$  are almost identical with the LUMO and LUMO + 1 of  $C_{80}$ , and similar resemblance is observed in the HOMO-4 of  $\text{Ce}_2@C_{80}$  and the LUMO + 2 of  $C_{80}$ . That is, the upper three levels of  $\text{Ce}_2@C_{80}$  are derived from the unoccupied molecular orbitals of  $C_{80}$  and electrons of the entrapped Ce atoms are transferred to these levels. Thus, the formal oxidation state of the fullerene can be described

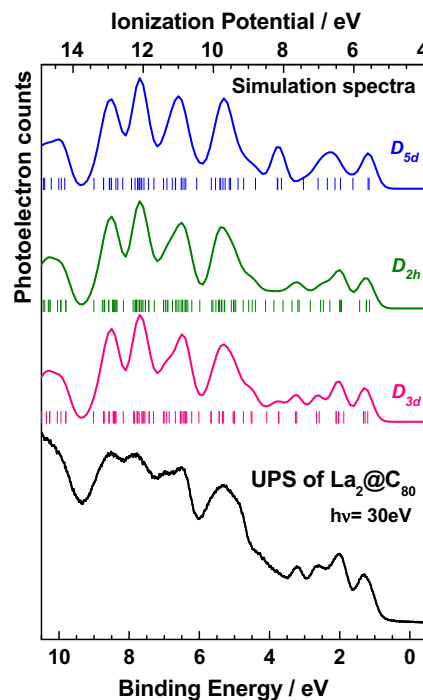
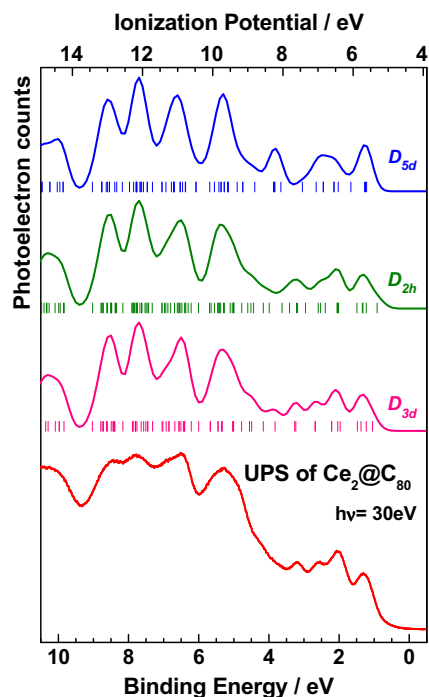
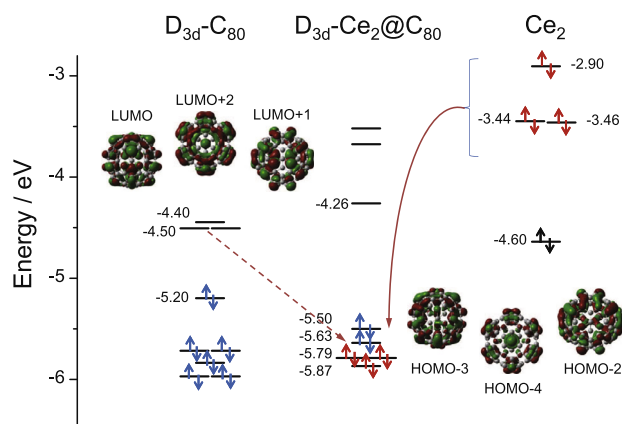


Fig. 4. The UPS of  $\text{La}_2@C_{80}$  obtained with 30 eV excitation photon and the simulated spectrum obtained by broadening of the Kohn–Sham orbital energies. Bars under each simulation spectrum indicate the energy of calculated ionization potentials. Three simulation spectra theoretically obtained from optimized geometry assuming  $D_{3d}$  cage symmetry. Details of geometry optimization are in the text.



**Fig. 5.** The UPS of  $\text{Ce}_2@C_{80}$  obtained with 30 eV excitation photon and the simulated spectrum obtained by broadening of the Kohn–Sham orbital energies. Bars indicate the Kohn–Sham orbital energies. Three simulation spectra theoretically obtained from optimized geometry assuming  $D_{3d}$  cage symmetry.



**Fig. 6.** Energy diagrams of empty  $C_{80}$ ,  $\text{Ce}_2@C_{80}$  obtained by DFT calculation. The Kohn–Sham orbital energies of frontier orbitals are inserted and the wave function distributions of frontier orbitals are also shown. The electron configuration of  $\text{Ce}_2@C_{80}$  could be  $(\text{Ce}_2)^{6+}@C_{80}^{6-}$ .

as  $\text{Ce}_2^+@C_{80}^{6-}$ . On the other hand, the HOMO-2 and HOMO-3 wave functions of  $\text{La}_2@C_{80}$  are almost identical with the LUMO and LUMO + 1 of  $C_{80}$ , and similar resemblance is observed in the HOMO-1 of  $\text{La}_2@C_{80}$  and the LUMO + 2 of  $C_{80}$ . That is, the upper three levels of  $\text{La}_2@C_{80}$  are derived from the unoccupied molecular orbitals of  $C_{80}$  and electrons of the entrapped La atoms are transferred to these levels. Thus, the formal oxidation state of the fullerene can be described as  $\text{La}_2^+@C_{80}^{6-}$ . Calculated charges of entrapped atoms are estimated by the natural population analysis (NPA). Presently obtained NPA charge of Ce atom in  $\text{Ce}_2@C_{80}$  is +2.21 and that of La atom in  $\text{La}_2@C_{80}$  is +2.31. The formal oxidation state of Ce and La atoms might be +3 and two atoms donates six electrons to the cage. The fullerene cage accepts the same amounts of the electrons from the entrapped atoms,  $\text{Ce}_2^+@C_{80}^{6-}$  and  $\text{La}_2^+@C_{80}^{6-}$ .

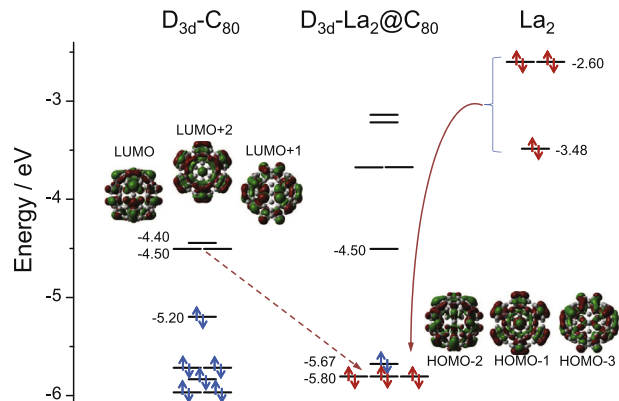


**Fig. 7.** Energy diagrams of empty  $C_{80}$ ,  $\text{La}_2@C_{80}$  obtained by DFT calculation. The Kohn–Sham orbital energies of frontier orbitals are inserted and the wave function distributions of frontier orbitals are also shown. The electron configuration of  $\text{La}_2@C_{80}$  could be  $(\text{La}_2)^{6+}@C_{80}^{6-}$ .

The empirical rule that the electronic structure of endohedral fullerenes depends on the cage structure and the amounts of transferred electrons holds in La or Ce atoms entrapped fullerenes.

#### 4. Conclusions

The intensity of the structures appearing in the UPS of  $\text{Ce}_2@C_{80}$  and  $\text{La}_2@C_{80}$  oscillates in accordance with the incident photon energy change, which means that this molecule has analogous geometry to other fullerenes. The UPS of  $\text{La}_2@C_{80}$  are the same as those of  $\text{Ce}_2@C_{80}$ , both have the same electronic structure. The UPS of  $\text{Ce}_2@C_{80}$  and  $\text{La}_2@C_{80}$  is well reproduced by the simulated spectrum obtained from the geometry optimized structure using DFT calculations, which indicates the validity of the geometry optimized structure. Comparison of the UPS with theoretically generated simulation spectra indicates that the most plausible structure of  $\text{Ce}_2@C_{80}$  and  $\text{La}_2@C_{80}$  has  $D_{3d}$  symmetry. Charge population analysis suggest  $\text{Ce}_2^+@C_{80}^{6-}$  and  $\text{La}_2^+@C_{80}^{6-}$  oxidation state.

#### Conflict of interest

There is no conflict of interest among authors.

#### Acknowledgments

This study was conducted as part of a Joint Research Program of UVSOR, Institute for Molecular Science. This work was supported by a Grant-in-Aid for Scientific Research in the Priority Area Molecular Conductors (No. 15073203) as well as a Grant-in-Aid for Basic Scientific Research (No. 18350068) from the Ministry of Education, Science, Sports, and Culture, Japan. This work is also supported by a Subsidy to Create Center of Excellence from Ehime University.

#### References

- [1] H. Shinohara, Rep. Prog. Phys. 63 (2000) 843, and references therein.
- [2] F.H. Hennrich, R.H. Michel, A. Fischer, S. Richard-Schneider, S. Gilb, M.M. Kappes, D. Fuchs, M. Biirk, K. Kobayashi, S. Nagase, Angew. Chem. Int. Ed. 35 (1996) 1732.
- [3] M.M. Alvarez, E.G. Gillan, K. Holczer, R.B. Kaner, K.S. Min, R.L. Whetten, J. Phys. Chem. 95 (1991) 10561.
- [4] T. Akasaka, S. Nagase, K. Kobayashi, M. Walchi, K. Yamamoto, H. Funasaku, M. Kato, T. Hoshino, T. Erata, Angew. Chem. Int. Ed. 36 (1997) 1643.
- [5] A.F. Hebard, M.J. Rosseinsky, R.C. Haddon, D.W. Murphy, S.H. Glarum, T.T.M. Palstra, A.P. Ramirez, A.R. Kortan, Nature 350 (1991) 600.
- [6] P.-M. Allemand, K.C. Khemani, A. Koch, F. Wudl, K. Holczer, S. Donovan, G. Gruner, J.D. Thompson, Science 253 (1991) 301.

- [7] E. Nishibori, M. Takata, M. Sakata, A. Taninaka, H. Shinohara, *Angew. Chem. Int. Ed.* 40 (2001) 2998.
- [8] K. Kobayashi, S. Nagase, T. Akasaka, *Chem. Phys. Lett.* 245 (1995) 230.
- [9] K. Kobayashi, S. Nagase, T. Akasaka, *Chem. Phys. Lett.* 261 (1996) 502.
- [10] H. Shimotani, T. Ito, Y. Iwasa, A. Aninaka, H. Shinohara, E. Nishibori, M. Takata, M. Sakata, *J. Am. Chem. Soc.* 126 (2004) 364.
- [11] J. Zhang, C. Hao, S. Li, W. Mi, P. Jin, *J. Phys. Chem. C* 111 (2007) 7862.
- [12] K. Muthukumar, J.A. Larsson, *J. Mater. Chem.* 18 (2008) 3347.
- [13] M. Yamada, T. Wakahara, T. Nakahodo, T. Tsuchiya, Y. Maeda, T. Akasaka, K. Yoza, E. Horn, N. Mizorogi, S. Nagase, *J. Am. Chem. Soc.* 128 (2006) 1402.
- [14] J. Ding, S. Yang, *Angew. Chem. Int. Ed. Engl.* 35 (1996) 2234.
- [15] T. Miyazaki, R. Sumii, H. Umemoto, H. Okimoto, Y. Ito, T. Sugai, H. Shinohara, S. Hino, *Chem. Phys.* 378 (2010) 11.
- [16] T. Miyazaki, R. Sumii, H. Umemoto, H. Okimoto, Y. Ito, T. Sugai, H. Shinohara, T. Zaima, H. Yagi, S. Hino, *Chem. Phys.* 397 (2012) 87.
- [17] T. Miyazaki, Y. Tokumoto, R. Sumii, H. Yagi, N. Izumi, H. Shinohara, S. Hino, *Chem. Phys.* 431–432 (2014) 47.
- [18] K. Iwasaki, S. Hino, D. Yoshimura, B. Cao, T. Okazaki, H. Shinohara, *Chem. Phys. Lett.* 397 (2004) 169.
- [19] S. Hino, N. Wanita, K. Iwasaki, D. Yoshimura, N. Ozawa, T. Kodama, K. Sakaguchi, H. Nishikawa, I. Ikemoto, K. Kikuchi, *Chem. Phys. Lett.* 402 (2005) 217.
- [20] S. Hino, N. Wanita, K. Iwasaki, D. Yoshimura, T. Akachi, T. Inoue, Y. Ito, T. Sugai, H. Shinohara, *Phys. Rev. B* 72 (2005) 195424.
- [21] S. Hino, T. Miyazaki, Y. Aoki, N. Wanita, M. Kato, R. Sumii, T. Akachi, T. Inoue, Y. Ito, T. Sugai, H. Shinohara, *Bull. Chem. Soc. Jpn.* 82 (2009) 963.
- [22] S. Hino, M. Zenki, T. Zaima, Y. Aoki, S. Okita, T. Ohta, H. Yagi, T. Miyazaki, R. Sumii, H. Okimoto, Y. Ito, H. Shinohara, *J. Phys. Chem. C* 116 (2012) 165.
- [23] S. Hino, K. Umishita, K. Iwasaki, T. Miyazaki, T. Miyamae, K. Kikuchi, Y. Achiba, *Chem. Phys. Lett.* 281 (1997) 115.
- [24] C.-R. Wang, T. Kai, T. Tomiyama, T. Yoshida, Y. Kobayashi, E. Nishibori, M. Takata, M. Sakata, H. Shinohara, *Nature* 408 (2000) 426.
- [25] T. Koga, S. Yamamoto, T. Shimazaki, H. Tatewaki, *Theor. Chem. Acc.* 108 (2002) 41.
- [26] Y. Osanai, M. Sekiya, T. Noro, T. Koga, *Mol. Phys.* 101 (2003) 65.
- [27] J. Binning, J.L. Martins, J.H. Weaver, P.F. Chibante, R.E. Smalley, *Science* 252 (1991) 1417.
- [28] T.R. Cummins, M. Burk, M. Schmidt, J.F. Armbruster, D. Fuchs, P. Adelman, S. Schupper, R.H. Michel, M.M. Kapps, *Chem. Phys. Lett.* 261 (1996) 228.